Results in Physics 42 (2022) 106009

Contents lists available at ScienceDirect

Results in Physics

journal homepage: www.elsevier.com/locate/rinp

High-performance detection of trace Hg^{2+} concentration enhanced by a functionalized optic-microfiber sensor

Dandan Sun [a,*], Yaohui Hao [a], Yongming Fu [a], Yukun Yang [b], Jie Ma [a,c,*]

[a] School of Physics and Electronic Engineering, Shanxi University, Taiyuan, China
[b] School of Life Science, Shanxi University, Taiyuan 030006, China
[c] School of Physics and Electronic Engineering, Collaborative Innovation Center of Extreme Optics, Shanxi University, Taiyuan, China

ARTICLE INFO

Keywords:
Optical spectroscopy
Optic-microfiber sensor
Hg^{2+} concentration
Functionalized film

ABSTRACT

The monitoring of heavy metal ions content has positive significance for water resources quality monitoring and environmental protection. Herein, a tapered microfiber sensor functionalized polydopamine/4-mercaptopyridine (PDA/4-MPY) film for detection of trace mercury ion (Hg^{2+}) concentration in water is proposed and demonstrated. The microfiber interferometer has excellent sensing performance including a refractive index (RI) sensitivity response of 1146 nm/RIU and a low-cross temperature response of −0.03 nm/℃. Hg^{2+} heavy metal ion is captured by the surface functional film to affect the RI of the microfiber surface, which lead to the wavelength shift of the interference spectrum. Experiments demonstrate that the sensor has an obvious regular response to Hg^{2+} in the range of 0–100 nM, in which the sensitivity reaches 1.015 nm/nM in the range of 0–10 nM with a high reliability ($R^2 = 0.99$). This sensor has high sensitivity response and strong specific recognition to trace Hg^{2+} concentration under the advantages of simple fabrication and low cost. Furthermore, the success of the proposed sensor also indicates that the combination of microfiber and nanomaterial has a bright prospect in the field of optical detection.

Introduction

As one of the most typical toxic heavy metal ions in nature, mercury ions (Hg^{2+}) exist widely in water environment and living organisms [1–3]. Hg^{2+} can be enriched into the human body through drinking water and food chains to cause a variety of diseases. Even the presence of trace amounts in the human body can also harm the digestive, kidney and central nervous system, and high levels can cause shock or even death [4–6]. In the face of this toxic heavy metal ion, the U.S Environmental Protection Agency and the World Health Organization limit the content of drinking water to no more than 10 nM and 30 nM, respectively [7,8]. Therefore, the proposal of Hg^{2+} sensor with high sensitivity, good selectivity and low detection limit has the vital practical value and significance for environmental protection and human safety.

According to previous studies, a variety of analytical techniques have been used for the detection of Hg^{2+} concentration. Cui et al. (2019) have proposed a colorimetric sensor based on covalent organic frameworks nanosheets for measuring Hg^{2+} concentration [5]. Ma et al. (2020) have detected Hg^{2+} concentration using a controlled release system electrochemical aptasensor combined with mesoporous silica nanocontainers [6]. Guo et al. (2020) have used Raman chip designed by modification of 4-pyridinethiol/gold nanoparticles/indium tin oxide film for measuring Hg^{2+} concentration [9]. Farideh et al. (2021) have proposed a Hg^{2+} sensor based on polymer nanofiber network and combined with anodic stripping voltammetry to determine Hg^{2+} concentration [10]. Selvaraj et al. (2021) have used fluorescence spectroscopy to measure the brightness of Hg^{2+} bound to tetraphenylethene derivative containing a mercury-binding moiety to obtain Hg^{2+} concentration [11]. The above studies fully reflect that the introducting nanotechnology has injected a new vitality into the development of optical and electrochemical detection technology. The addition of nanotechnology also greatly increases the sensitivity and specificity of the detection results. However, the fluorescence, electrochemistry, Raman and other techniques used above usually require expensive specialized equipment, complex synthesis of chemical reagents and professional knowledge of operating instruments [5,6,9–11], which virtually increases the cost and difficulty of the experiment.

According to previous studies, as a kind of developable multifunction platform, a variety of optical fiber sensing techniques have been used to detect the concentration of heavy metal ions because of its

* Corresponding authors at: School of Physics and Electronic Engineering, Shanxi University, Taiyuan, China (D. Sun, J. Ma).
E-mail addresses: sundd@sxu.edu.cn (D. Sun), mj@sxu.edu.cn (J. Ma).

https://doi.org/10.1016/j.rinp.2022.106009
Received 15 July 2022; Received in revised form 6 September 2022; Accepted 19 September 2022
Available online 21 September 2022

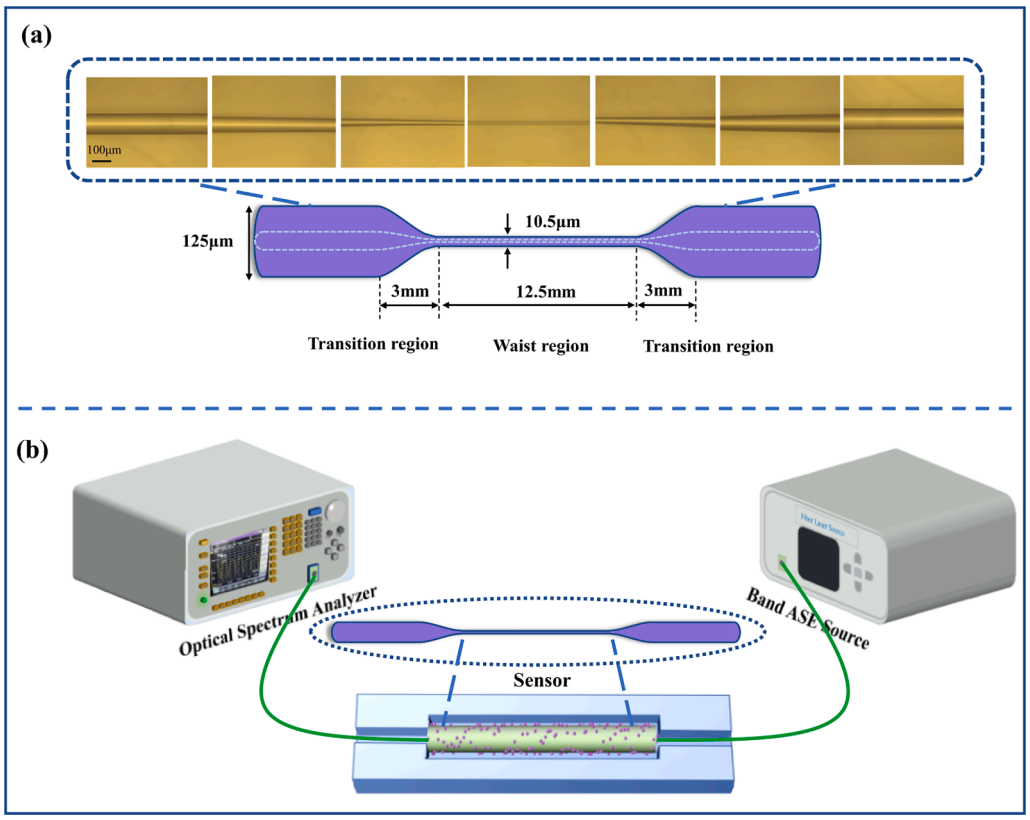

Fig. 1. (a) Schematic diagram of tapered microfiber interferometer structure with parameters (the insets are the SEM morphology); (b) Schematic diagram of microfiber sensor detection system.

unique advantages of small size, light weight, electromagnetic immunity, and high sensitivity [12–14]. Kishore et al. (2017) have used fiber Bragg grating sensor combined with hydrogel coating with expansion ability to measure the concentration of chromium ion (Cr^{6+}) solution [15]. Zhang et al. (2018) have used a interferometer fiber sensor composed of fiber Bragg grating, coreless fiber and chitosan/polyacrylic acid sensitive film to measure the Hg^{2+} concentration [16]. Sadani et al. (2019) have proposed a U-bend optical fiber immobilized chitosan capped gold nanoparticles for trace detection of Hg^{2+} in diverse matrices [17]. Yin et al. (2019) have developed a microfiber coil resonator based on black phosphorus to detect lead ions (Pb^{2+}) in water [18]. Yuan et al. (2019) have used a fiber-optic surface plasmon resonance sensor by forming a sandwich structure to detect the Hg^{2+} concentration [4]. Liu et al. (2019) have used optical fiber fluorescence sensors to measure the Hg^{2+} concentration by measuring the quenching degree of luminescent quantum dots on the surface of tapered optical fiber probe after binding to Hg^{2+} [19]. Acha et al. (2020) have used the aptamer-based tapered fluorescent fiber sensor to detect the Hg^{2+} concentration in water [20]. Yi et al. (2022) have achieved the measurement of nickel ions (Ni^{2+}) concentration in the 10–100 nM range by using a tapered microfiber sensor coated with an ion-imprinted chitosan polymer [21]. The optical fiber sensors mentioned above have made great achievements in the field of heavy metal ion detection by virtue of their unique structures and materials. However, the fabrication of grating devices require the expensive femtosecond laser, a carbon dioxide laser or 193/248 nm excimer ultraviolet laser. The fiber-optic surface plasmon resonance sensors usually need precious metal nanoparticles and complex sandwich structures and fiber-optic fluorescence sensors are particularly sensitive to the interference. In order to solve this series of problems, as a typical representative of optic-fiber device, the tapered microfiber interferometer is considered to be a promising sensor for object concentration analysis due to its super evanescent wave, simple fabrication, low cost and ultra-high sensitivity [12,13,22]. The sensitivity and specificity of the sensor can be further improved by adding the polymer coating that can specifically bind to the molecule to be measured on the surface of microfiber, which further broadens the application field and practical value of microfiber [13,14,22,23]. The interaction between the sensitive material and the object to be measured will affect the characteristics of the output light, which makes the biological and chemical signals converted into optical signals through the microfiber sensor [24].

The polydopamine (PDA) is a kind of biomolecular material with strong adhesion ability similar to mussel adhesion protein, which is a dark brown colloid formed by self-polymerization of dopamine (DA) in alkaline buffer and aerobic environment [25,26]. PDA is often used as a biofilm to modify solid materials because of its easy and uniform adhesion to the surface of various solid materials [27,28]. In particular, PDA contains a large number of amino, hydroxyl, catechol and other active groups, which can be coupled with molecules containing sulfhydryl (-SH) and amino groups through Michelson or Schiff base reaction to achieve further modification [13,28–30]. 4-mercaptopyridine (4-MPY) is selected as a suitable intermediate material, the -SH of 4-MPY can be coupled with DA and its pyridine nitrogen (N) can combine with detected Hg^{2+} to form stable $Hg(MPY)_2$ complex via multidentate *N*-bonding [4,9,31], which provides practical value for the subsequent microfiber sensor to detect the Hg^{2+} concentration.

In this work, a tapered microfiber interferometer functionalized PDA/4-MPY film is proposed to detect Hg^{2+} concentration with high sensitivity and selectivity. With its unique conical structure and ultrafine diameter, the microfiber interferometer has excellent sensing performance including a refractive index (RI) sensitivity response of 1146 nm/RIU and a low-cross temperature response of −0.03 nm/℃. The PDA/4-MPY film functionalized sensor realized by one step dip-coating method. Subsequent experiments and analysis demonstrate that this proposed sensor has a obvious response of Hg^{2+} detecting concentration at 0–100 nM with a high sensitivity of 1.015 nm/nM in the range of

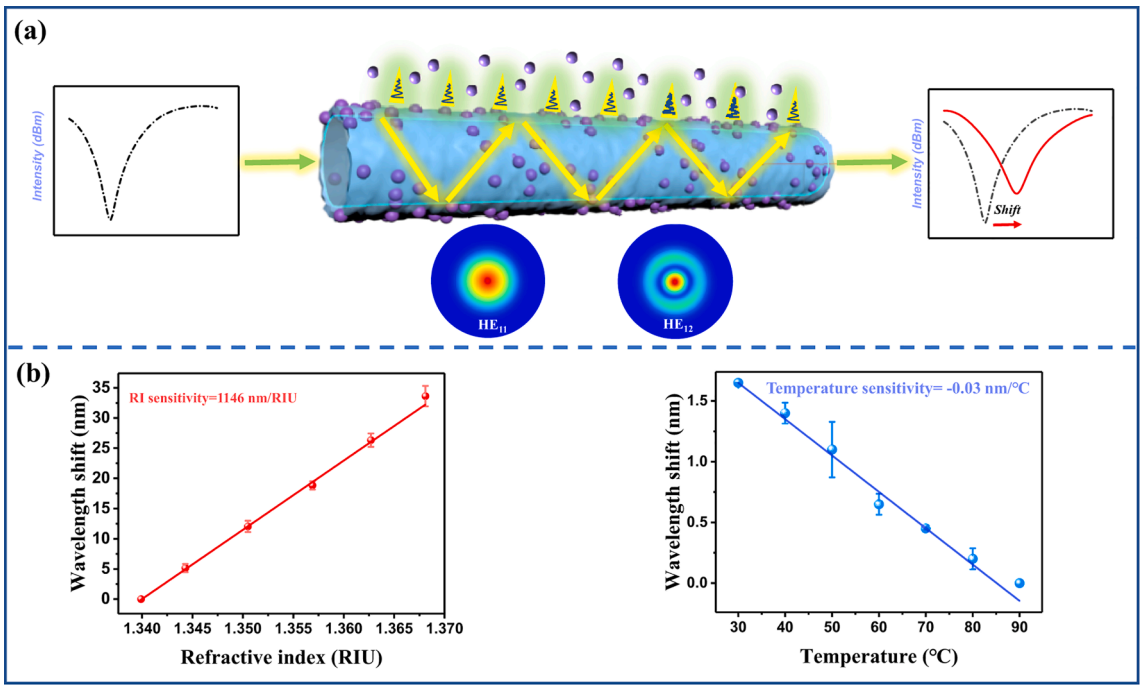

Fig. 2. (a) Principle diagram of microfiber sensor for Hg^{2+} concentration detection (the insets are the transverse electric field amplitude distribution of HE_{11} and HE_{12} in the major interference modes); (b) RI and temperature response of the microfiber interferometer with error bar.

0–10 nM. In addition, it is confirmed that the sensor has a good specific recognition of Hg^{2+}. The proposed sensor has positive significance for Hg^{2+} concentration analysis and quality monitoring protection in water environment. Meanwhile, the platform of microfiber device functionalized with sensitive materials is also expected to exert its potential strength in more applications in the future.

Experimental section

Reagents and instruments

Dopamine hydrochloride (DA, 98 %), tromethane hydrochloride buffer (Tris-HCl, 1.0 M, pH8.5), 4-Mercaptopyridine (4-MPY, 96 %), mercury nitrate monohydrate ($Hg(NO_3)_2{\cdot}H_2O$, 99.5 %), aluminum chloride ($AlCl_3$, 99 %), nickel chloride ($NiCl_2$, 99 %), sodium chloride (NaCl, 99.5 %), calcium chloride ($CaCl_2$, 99.99 %), copper chloride ($CuCl_2$, 98 %), ferrous chloride ($FeCl_2$, 99.5 %) and lead chloride ($PbCl_2$, 99.5 %) were purchased from Shanghai Macklin Biochemical Technology Co., ltd. (Shanghai, China). Tris-HCl buffer was used to dissolve DA and 4-MPY. Deionized water (DI) was used to dissolve the tested solutions of heavy metal ions.

The instruments used in the experimental testing process included an amplified spontaneous emission (ASE) light source and an optical spectrum analyzer (OSA, Anritsu MS9740A, Japan). In addition, the instruments used in preparation and analysis process included digital refractometry (Reichert 13940000), optical fiber fusion splicer (Fujikura FSM-60S, Japan), temperature incubator (HT-330, China), 3D Printers (DDKUN, China), electronic analytical balance (LICHEN FA1004, China), scanning electron microscopy (SEM, ZEISS SIGMA 300, Germany), energy dispersion X-ray (EDX, Ultim Extreme, Britain) spectrometer, Raman spectrometer (Thermo DXR2xi, USA) and metallographic microscope (Caikon DMM-200C, China).

Sensor fabrication

Firstly, a special optical fiber (germanium-doped silica fiber) with a length of 2–3 cm was connected between two ordinary single-mode optical fibers by fiber fusion machine. The microfiber interferometer was fabricated by the fused taper technology, which required the special optical fiber to be fixed on a stretchable displacement platform, and then stretched a certain distance at a uniform speed after 5 s burning by butane flame [32,33]. In order to balance the stability and sensitivity of the sensor, we made a microfiber with special parameters as shown in Fig. 1a. It was observed that the tapered microfiber sensor included a uniform area with a length of 12 mm and a diameter of 10.5 μm and two transition areas with a length of 3 mm. The insets were the real map of each part of the tapered microfiber by the metallurgical microscopy.

Experimental facility

The diagram of the experimental device was shown in Fig. 1b. The light within the range of 1528–1603 nm emitted by a band ASE light source was transmitted to an OSA with a resolution of 0.03 nm. The fabricated microfiber interferometer between the two devices to form the interference spectrum, which was detected by OSA apparatus. To ensure that the volume of the tested solution was the same and the solution wasn't easy to flow out by testing, the sensor was placed in a special concave groove that widths of 5 mm and 2 mm on the middle and sides, and the depth of the groove is 2 mm.

Sensing Principle

The non-adiabatic tapered microfiber realized the Mach–Zehnder interferometer (MZI) because of its three special regions: down-taper, up-taper and uniform region. The mode leakage occured when the light passed through the one taper region, which excites the high-order mode. The fundamental mode and the high-order mode were transmitted through the uniform region together. Due to the significant difference in the RI inside and outside the microfiber, the fundamental mode and the high-order mode were coupled together to produce interference fringes when transmitted to the other taper region [34–36]. RI sensitivity is an important parameter to measure the performance of microfiber sensor and it represents the influence of the change of external refractive index of microfiber on the wavelength of interference

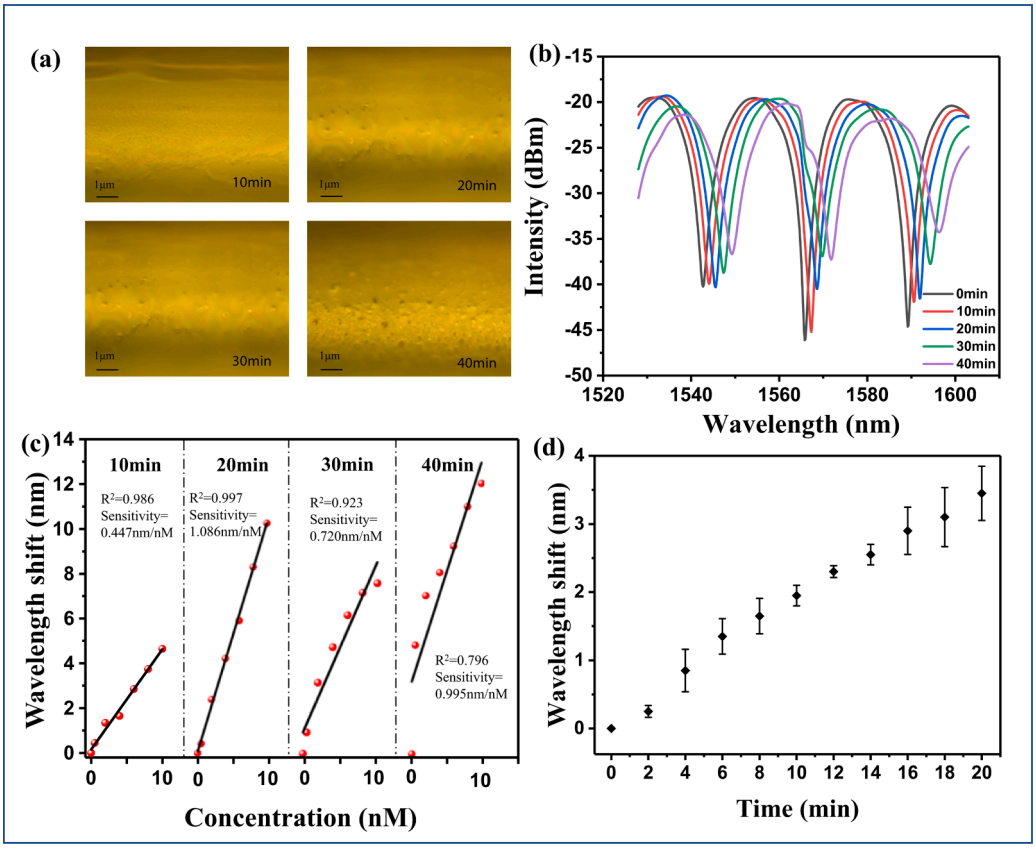

Fig. 3. (a) The metallographic microscopic images and (b) the spectral variation of the microfiber interferometer immersed in PDA/4-MPY mixed solution after 10, 20, 30 and 40 min respectively; (c) Linear response of the sensor to Hg^{2+} concentration in the range of 0–10 nM after soaking in PDA/4-MPY solution for different times; (d) The wavelength shift of the interference spectrum after the microfiber interferometer immersed in PDA/4-MPY mixed-solution for 20 min.

spectrum. It can be expressed by the following formula [13,32,33,37]:

$$s = \frac{d\lambda}{dn_{med}} = \frac{\lambda}{\Gamma}\left(\frac{1}{\Delta n_{eff}}\frac{d\Delta n_{eff}}{dn_{med}}\right) \quad (1)$$

where $\Gamma = 1 - \frac{\lambda}{\Delta n_{eff}}\frac{d\Delta n_{eff}}{d\lambda}$ is the dispersion factor, which represents the effect of RI difference with wavelength and is typically negative in microfiber systems. where n_{med} denotes the RI of the medium, which is the RI of the PDA/4-MPY film in the experiment. dn_{med} is the RI change of the medium, and its small change can affect the change of the interference wavelength. Due to the special structure of the tapered microfiber interferometer, mode coupling and reorganization will occur in the taper region, among which the main modes are fundamental HE_{11} and high-order HE_{12} modes, as shown in the illustration in Fig. 2a. Δn_{eff} is the mode index difference between HE_{11} and HE_{12} modes and $d\Delta n_{eff}/dn_{med}$ is the RI-induced variation of the index dependence. Although the exponent of both the HE_{11} and HE_{12} modes increases as the RI of the external environment increases, the exponent of the HE_{11} mode increases less than that of the HE_{12} mode, so $d\Delta n_{eff}/dn_{med}$ is a negative value. Based on the above analysis, it can be concluded that S is positive, indicating that the wavelength of the interference spectrum will be redshifted with the increase of the RI of the external medium. After the detected Hg^{2+} is captured by the 4-MPY film on the surface of the microfiber sensor, the RI of the external medium would increase and the interference wavelength will be redshifted, as shown in Fig. 2a.

In addition to the influence of the RI change in the external medium on the RI sensitivity, the RI sensitivity is closely related to the diameter of the microfiber. The smaller diameter of the microfiber provides stronger evanescent field resulting in higher RI sensitivity [32,34,37].

Results and discussion

Basic sensing performance

High RI sensitivity and low-cross temperature response are two key indexes to evaluate the sensor performance. In order to accurately measure the RI response of the sensor, the sodium chloride solution with different RI is measured through the above experimental apparatus. After each measurement, the sensor is cleaned with DI water and the next measurement is carried out after the spectrum returned to its initial position in the air. The good repeatability of the RI response of the sensor is verified by three times experiments using the same microfiber interferometer. The RI response is obtained by analyzing and fitting the position change of interference spectrum dip. Fig. 2b (left) shows a linear fitting diagram of the RI response of the microfiber interferometer with error bar, which shows that the sensor has a RI sensitivity up to 1146 nm/RIU with minimal error.

The low-cross temperature response can minimize the interference caused by the temperature change in the testing process. The fabricated microfiber interferometer is placed in a custom thermostat, and the temperature response of the microfiber interferometer is obtained by analyzing the change of the dip position of the interference spectrum as the increase of temperature. Fig. 2b (right) shows the linear fitting diagram of the temperature response of the microfiber interferometer under the repeated measurement results. It can be seen from the diagram that the microfiber interferometer has an extremely low-cross temperature response and the sensitivity is −0.03 nm/°C within the range of 30–90 °C.

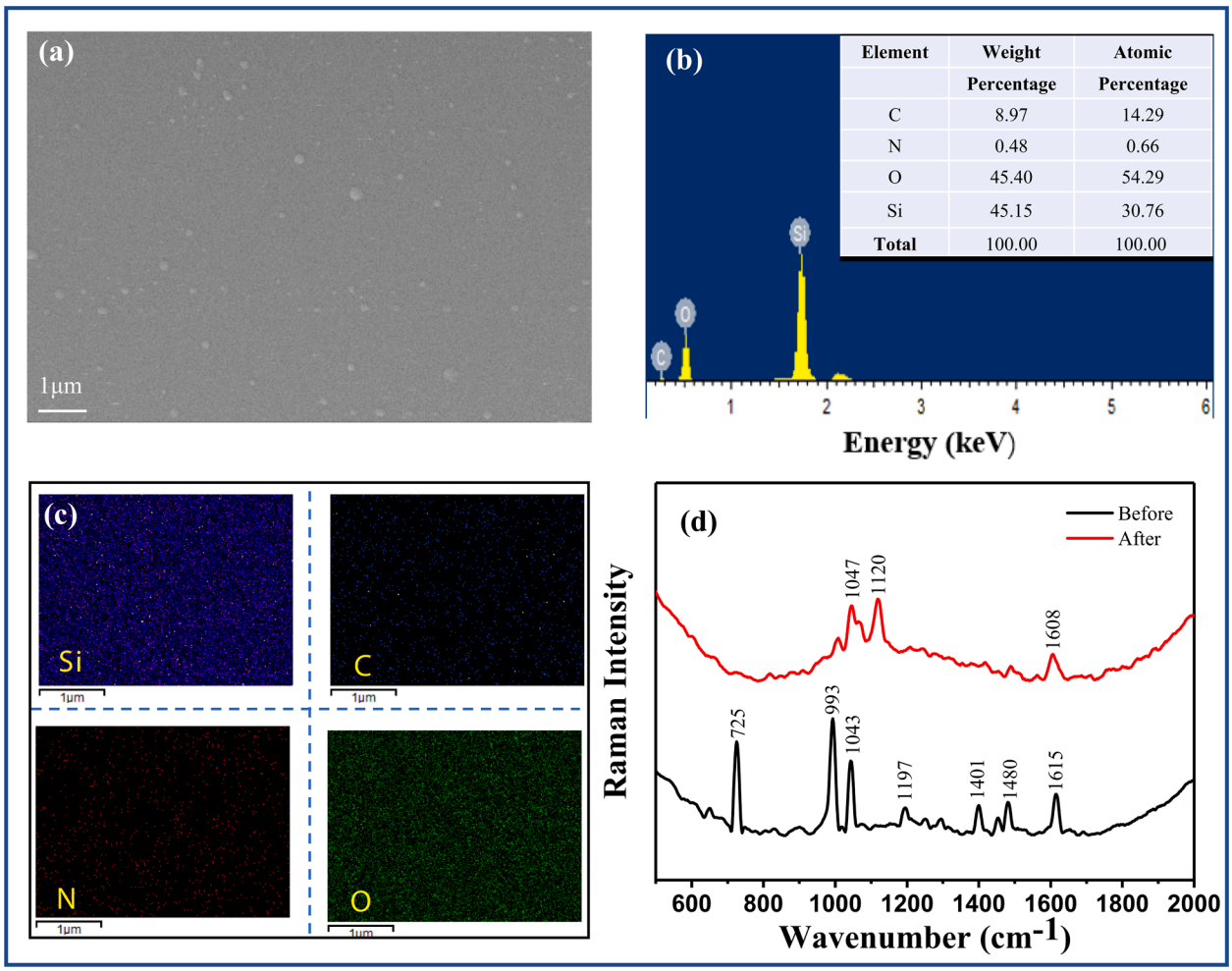

Fig. 4. (a) SEM characterization of the fiber coated with PDA/4-MPY film; (b) EDX analysis (the inserted table is element content analysis) with (c) the mapping analysis; (d) The Raman spectra of 4-MPY film before and after Hg^{2+} binding.

Sensor characterization

The reasonable combination of nano-material layer and microfiber interferometer under specific conditions is the highest priority to obtain the functional sensor. 0.2 g hydrochloride DA powder is dissolved by 100 mL Tris-HCl buffer to form 2 g/L PDA solution, which is stirred for 1 h in an aerobic environment to obtain PDA solution through self-polymerization [13,25,38,39]. Then 0.12 g 4-MPY is added to PDA solution. PDA/4-MPY mixed solution is formed by Michelson addition reaction between the 4-MPY and PDA [29,30]. The nano-material layer composed of PDA/4-MPY mixed-solution is uniformly coated on the surface of optical fiber by the one step dip-coating method [13,38,40]. The choice of soaking time is the key factor for forming a uniform film. Fig. 3a shows the metallographic microscopic images of optical fibers soaked in PDA/4-MPY mixed-solution for 10, 20, 30 and 40 min respectively, which indicates that the coating layer formed under 20 min is denser than that formed under 10 min, and similar to that formed under 30 and 40 min. Fig. 3b shows the spectral variation of the microfiber interferometer immersed in PDA/4-MPY mixed solution with soaking time, from which it can be seen that soaking for a longer time may deteriorate the spectra and increase losses. Fig. 3c shows the linear response of the sensor to Hg^{2+} concentration in the range of 0–10 nM after soaking in PDA/4-MPY solution for different times. It can be seen from the Fig. 3c that the sensitivity and accuracy of the response at the time of soaking for 20 min are much higher than those at other times. Fig. 3d shows the wavelength transfer diagram of the interference spectrum after the sensor immersed in PDA/4-MPY mixed-solution for 20 min in the repeated measurement results, which shows that the wavelength is about red-shifted 3.5 nm after 20 min. Therefore, as the optimal time condition, 20 min is finally chose to form a uniform film coating on the surface of microfiber interferometer under the trade-off between the best effect and the production time cost [13,38].

The surface morphology and chemical composition of the fiber coated with PDA/4-MPY materials film are confirmed by SEM with EDX spectroscopy analysis, and the result is shown in Fig. 4. Fig. 4a shows the SEM diagram of fiber with material layer. Fig. 4b shows the results of elemental analysis on the surface of the fiber, in which the presence of element N indicates the successful attachment of the PDA/4-MPY material layer [41]. Fig. 4c is the mapping analysis of corresponding Si, C, N and O elements. Fig. 4d shows the Raman spectra of 4-MPY film before and after Hg^{2+} binding. By using Raman spectrometer with excitation wavelength of 532 nm for testing sample in Fig. 4d, it can be seen that the Raman spectrum peak value of 4-MPY reveals at 1043 and 1615 cm^{-1} (black line). The coordination of mercury ions with pyridine nitrogen (N) will disturb the electron distribution between the different bonds in the aromatic ring of 4-MPY, which causes the peak attenuation and shift of the Raman spectra of 4-MPY at 1047,1608 cm^{-1} (red line) [9,42–44]. Thus, the specific binding mechanism between 4-MPY and Hg^{2+} can provide a strong guarantee for the Hg^{2+} concentration detection in subsequent experiments.

Hg^{2+} concentration detection

Fig. 5a shows the schematic diagram of Hg^{2+} concentration

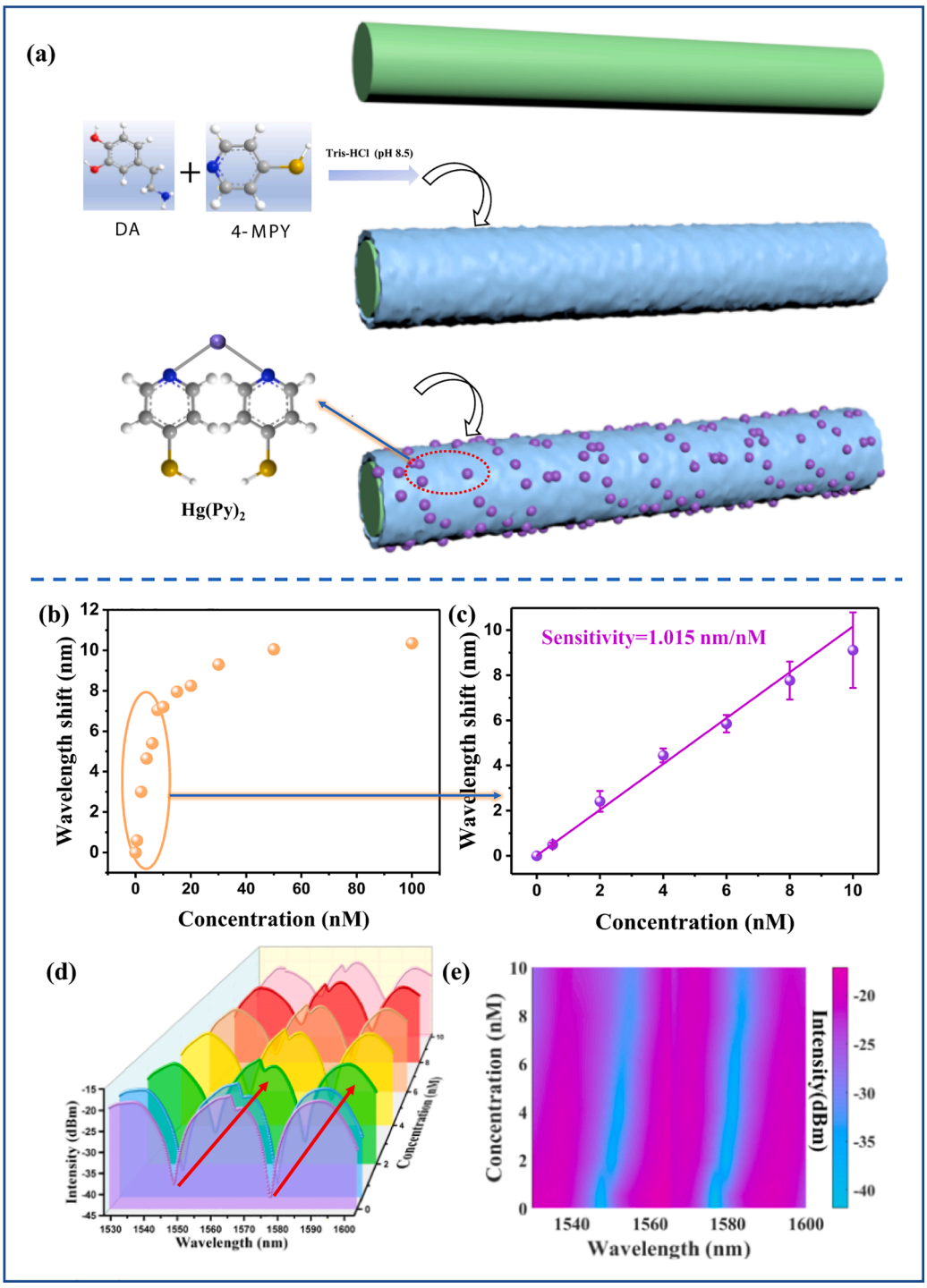

Fig. 5. (a) The schematic diagram of Hg^{2+} concentration detection by PDA/4-MPY film functionalized microfiber sensor; (b) The response of the sensor to Hg^{2+} in the range of 0–100 nM; (c) The linear response of the sensor to Hg^{2+} in the low range of 0–10 nM; (d) The shift of the corresponding interference spectrum; (e) The wavelength response of the interference spectrum.

detection by PDA/4-MPY film functionalized microfiber sensor. The experiment is mainly divided into two steps: the fabrication of functionalized microfiber sensor and the detection of Hg^{2+} concentration. Firstly, the PDA/4-MPY mixed solution is poured into the chip with microfiber interferometer, and the solution is removed after soaking the fiber for 20 min. By means of natural deposition, a layer of PDA/4-MPY material film is successfully functionalized by one step dip-coating method growth on the surface of the microfiber interferometer depending on the adhesion of PDA [13,27,28]. Secondly, the Hg^{2+} solution is flowed into the chip in the order from low to high concentration and the corresponding interference spectrum at each concentration is recorded. $(Hg(NO_3)_2{\cdot}H_2O$ powder is dissolved with DI water to obtain Hg^{2+} solutions with different concentrations of 0, 0.5, 2, 4, 6, 8, 10, 15, 20, 30, 50 and 100 nM. The pyridine N of 4-MPY can combine with detected Hg^{2+} to form stable $Hg(MPY)_2$ complex via multidentate *N*-bonding [4,9,31], which will affect the RI of external medium of microfiber interferometer, and finally reflect the concentration of Hg^{2+} solution through the deviation of interference spectrum wavelength.

Fig. 5b shows the detection results of Hg^{2+} concentration in the range of 0–100 nM, and indicates that the interference spectrum

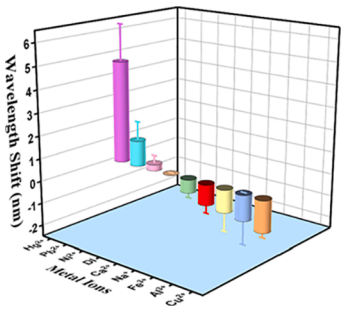

Fig. 6. Response of the PDA/4-MPY film functionalized micorfiber sensor to different heavy metal ions (Hg^{2+}, Pb^{2+}, Ni^{2+}, Ca^{2+}, Na^{+}, Fe^{3+}, Al^{3+}, Cu^{2+}).

redshifts with the increase of Hg^{2+} concentration and the detection curve gradually becomes saturated at 30 nM. The main reason for this phenomenon is that the surface area of microfiber interferometer itself is limited and the film attached to the surface also has a certain limit. Through three experiments and error analysis under the same steps and conditions, the linear fitting curve is obtained as shown in Fig. 5c. In detail, the response of the functional microfiber sensor to Hg^{2+} in the low range of 0–10 nM with error bar (standard deviation) is exhibited, which has the detection sensitivity of 1.105 nm/nM. Fig. 5d shows the shift of the corresponding interference spectrum, and it is obvious that the interference spectrum drifts to the direction of wavelength increase. Fig. 5e shows the wavelength response of the interference spectrum. Combining all the above analysis and testing results, it can be concluded that the response of PDA/4-MPY functionalized microfiber sensor to Hg^{2+} has high accuracy and good repeatability.

Selectivity property

Whether the sensor has specific response to the object to be tested is one of the important criteria to judge the sensor is qualified or not. In order to verify the selectivity property of this sensor, the functionalized microfiber sensor tested on different heavy metal ions in the concentration range of 0–10 nm for three times according to the experimental schematic diagram in Fig. 1b and the Hg^{2+} detecting procedure in Fig. 5a. Fig. 6. show that response of the PDA/4-MPY film functionalized microfiber sensor to different heavy metal ions (Hg^{2+}, Pb^{2+}, Ni^{2+}, Ca^{2+}, Na^{+}, Fe^{3+}, Al^{3+}, Cu^{2+}) at the standard of zero response to DI. It can be seen from the figure that the response of the sensor to Hg^{2+} metal ion is much higher than that of other heavy metal ions, indicating that the sensor has a good specific recognition effect for Hg^{2+} metal ion.

Table 1 shows a comparison of this work with some currently popular methods for detecting Hg^{2+} concentration using optical fibers. Under the condition of simple fabrication and low cost, the functionalized microfiber sensor can also accurately detect Hg^{2+} concentration in the range of low concentration, which fully reflects the advantage of the PDA/4-MPY functionalized microfiber sensor realized by one-step synthesis method to respond to trace Hg^{2+}.

Conclusions

In this work, a tapered microfiber interferometer functionalized PDA/4-MPY film is proposed to detect Hg^{2+} concentration with high sensitivity and selectivity. The microfiber sensor has excellent sensing performance including a RI sensitivity response of 1146 nm/RIU and a low-cross temperature response of −0.03 nm/℃. The realization of functionalized film adopts by one step dip-coating method. Experiments demonstrate that the sensor has an obvious regular response to Hg^{2+} in the range of 0–100 nM, in which the sensitivity reaches 1.015 nm/nM in the range of 0–10 nM with a high reliability ($R^2 = 0.99$). The detection concentration of the sensor is lower than the standards specified by U.S Environmental Protection Agency and the World Health Organization, which means that the performance of the sensor can meet the Hg^{2+} concentration detection in highly demanding environments. The proposed sensor has important implications for water resource quality detection and environmental protection, and broadens the application field of microfiber platform, which has great practical guiding significance for the combination of nanomaterials and optical detecting technology.

CRediT authorship contribution statement

Dandan Sun: Conceptualization, Methodology, Data curation, Writing – original draft. **Yaohui Hao:** Conceptualization, Methodology, Data curation, Writing – original draft, Writing – review & editing. **Yongming Fu:** Validation, Investigation, Supervision, Writing – review & editing. **Yukun Yang:** Validation, Investigation, Supervision, Writing – review & editing. **Jie Ma:** Validation, Investigation, Supervision, Writing – review & editing.

Declaration of Competing Interest

The authors declare that they have no known competing financial interests or personal relationships that could have appeared to influence the work reported in this paper.

Table 1
Comparison of previous studies on Hg^{2+} detection by fiber optic sensors.

Methods	Main chemical materials	Linear range	Sensitivity	detection limit	Manufacturing difficulty	Cost	Reference
Fiber-optic surface plasmon resonance	AuNPs/4-MPY	8–100 nM	–	8 nM	Medium	High	[4]
No-core fiber combined with a fiber Bragg grating	Silver film and chitosan/poly acrylic acid	0–100 μM/ 100–500 μM	0.0823 nm/ μM/ 0.0178 nm/ μM	25 μM	Difficult	High	[16]
U-bend optical fiber surface plasmon resonance	Chitosan capped gold nanoparticles	0.1–540 ppb (0.5–2700 nM)	–	0.1 ppb (0.5 nM)	Medium	High	[17]
Luminescent Optical Fiber	Nucleic acid aptamer	$5x10^{-3}$-0.5 nM	–	$5x10^{-3}$ nM	Difficult	High	[20]
Reflective fiber surface plasmon resonance	Chitosan/polyacrylic acid	0–30 μM/ 30–100 μM/ 100–200 μM	0.5586 nm/ μM 0.1239 nm/ μM 0.02 nm/μM	μM scale	Difficult	Medium	[45]
U-bend optical fiber surface plasmon resonance	Escherichia coli/gold nanoparticles	0.5–2000 ppb (2.5–10000 nM)	0.08065a.u./ ppb	0.5 ppb (2.5 nM)	Difficult	High	[46]
Tapered microfiber interferometer	PDA/4-MPY	0.5–10 nM	1.105 nm/nM	0.2 nM	Easy	Low	This work

Data availability

Data will be made available on request.

Acknowledgments

This work was supported by the National Natural Science Foundation of China (62005147, 61722507, 61901249, 32072301); the International Cooperation and Exchange of the National Natural Science Foundation of China (62020106014).

References

[1] Wang L, Chen H, Zhang N, Liu X, Zheng K. Reaction-based two novel fluorescent probes for Hg^{2+} detection using benzothiazole derivatives via ESIPT mechanism in aqueous solution and serum. Tetrahedron Lett 2021;64:152735.
[2] Lai C, Liu S, Zhang C, Zeng G, Huang D, Qin L, et al. Electrochemical Aptasensor Based on Sulfur-Nitrogen Codoped Ordered Mesoporous Carbon and Thymine-Hg^{2+}-Thymine Mismatch Structure for Hg^{2+} Detection. ACS Sens 2018;3(12):2566–73.
[3] Zhao X, Campbell S, El-Khoury PZ, Jia Y, Wallace GQ, Claing A, et al. Surface-Enhanced Raman Scattering Optophysiology Nanofibers for the Detection of Heavy Metals in Single Breast Cancer Cells. ACS Sens 2021;6(4):1649–62.
[4] Yuan H, Ji W, Chu S, Liu Q, Qian S, Guang J, et al. Mercaptopyridine-Functionalized Gold Nanoparticles for Fiber-Optic Surface Plasmon Resonance Hg^{2+} Sensing. ACS Sens 2019;4(3):704–10.
[5] Cui W-R, Zhang C-R, Jiang W, Liang R-P, Wen S-H, Peng D, et al. Covalent Organic Framework Nanosheet-Based Ultrasensitive and Selective Colorimetric Sensor for Trace Hg^{2+} Detection. ACS Sustainable Chem Eng 2019;7(10):9408–15.
[6] Ma N, Ren X, Wang H, Kuang X, Fan D, Wu D, et al. Ultrasensitive Controlled Release Aptasensor Using Thymine-Hg^{2+}-Thymine Mismatch as a Molecular Switch for Hg^{2+} Detection. Anal Chem 2020;92(20):14069–75.
[7] Song XL, Fu BC, Lan YF, Chen YX, Wei YL, Dong C. Label-free fluorescent aptasensor berberine-based strategy for ultrasensitive detection of Hg^{2+} ion. Spectrochim Acta Part A Mol Biomol Spectrosc 2018;204:301–7.
[8] Duan YF, Zhang Y, Wang F, Sun YT, Chen M, Jing Z, et al. 4-Mercaptopyridine Modified Fiber Optic Plasmonic Sensor for Sub-nM Mercury (II) Detection. Photonic Sens 2021;12(1):1–8.
[9] Guo X, Chen Fu, Wang F, Wu Y, Ying Ye, Wen Y, et al. Recyclable Raman chip for detection of trace Mercury ions. Chem Eng J 2020;390:124528.
[10] Narouei FH, Livernois L, Andreescu D, Andreescu S. Highly sensitive mercury detection using electroactive gold-decorated polymer nanofibers. Sens Actuators B Chem 2021;329:129267.
[11] Selvaraj M, Rajalakshmi K, Ahn D-H, Yoon S-J, Nam Y-S, Lee Y, et al. Tetraphenylethene-based fluorescent probe with aggregation-induced emission behavior for Hg^{2+} detection and its application. Anal Chim Acta 2021;1148:238178.
[12] Lu JY, Yu Y, Qin SP, Li MW, Bian Q, Lu Y, et al. High-performance temperature and pressure dual-parameter sensor based on a polymer-coated tapered optical fiber. Opt Express 2020;30(6):9714–26.
[13] Wang M, Dai S, Gan N, Wang Y. In situ growth of silver nanoparticles on polydopamine-coated chalcogenide glass tapered fiber for the highly sensitive detection of volatile organic compounds in water. J Non-Cryst Solids 2022;581:121420.
[14] Zhang H, Cong B, Zhang F, Qi Y, Hu T. Simultaneous measurement of refractive index and temperature by Mach-Zehnder cascaded with FBG sensor based on multi-core microfiber. Opt Commun 2021;493:126985.
[15] Kishore PVN, Shankar MS, Satyanarayana M. Detection of trace amounts of chromium(VI) using hydrogel coated Fiber Bragg grating. Sens Actuators B Chem 2017;243:626–33.
[16] Zhang YN, Zhang LB, Han B, Gao P, Wu QL, Zhang AZ. Reflective mercury ion and temperature sensor based on a functionalized no-core fiber combined with a fiber Bragg grating. Sens Actuators B Chem 2018;272:331–9.
[17] Sadani K, Nag P, Mukherji S. LSPR based optical fiber sensor with chitosan capped gold nanoparticles on BSA for trace detection of Hg (II) in water, soil and food samples. Biosens Bioelectron 2019;134:90–6.
[18] Yin Yu, Li S, Wang S, Jia S, Ren J, Farrell G, et al. Ultra-high-resolution detection of Pb^{2+} ions using a black phosphorus functionalized microfiber coil resonator. Photonics Res 2019;7(6):622.
[19] Liu T, Wang W, Jian D, Li J, Ding He, Yi D, et al. Quantitative remote and on-site Hg^{2+} detection using the handheld smartphone based optical fiber fluorescence sensor (SOFFS). Sens Actuators B Chem 2019;301:127168.
[20] Acha ND, Elosúa C, Arregui FJ. Development of an Aptamer Based Luminescent Optical Fiber Sensor for the Continuous Monitoring of Hg^{2+} in Aqueous Media. Sensors 2020;20(8):2372.
[21] Yi Z, Liu J, Liu B, Guo H, Wu Q, Shi J, et al. Optical microfiber sensor for detection of Ni^{2+} ions based on ion imprinting technology. Analyst 2022;147(2):358–65.
[22] Zhao Y, Liu J, Li H, Xu M, Li J, Jing C, et al. An ultra-sensitive gas pressure sensor based on tapered fiber coated with PDMS film working at TAP. Opt Laser Technol 2022;151:107998.
[23] Yap SHK, Chan KK, Zhang Z, Tjin SC, Yong KT. Carbon Dot-functionalized Interferometric Optical Fiber Sensor for Detection of Ferric Ions in Biological Samples. ACS Appl Mater Interfaces 2019;11(31):28546–53.
[24] Martínez-Hernández ME, Goicoechea J, Arregui FJ. Hg^{2+} Optical Fiber Sensor Based on LSPR Generated by Gold Nanoparticles Embedded in LBL Nano-Assembled Coatings. Sensors 2019;19(22):4906.
[25] Wang PL, Zhou YL, Wen Y, Wang F, Yang HF. In situ polydopamine-assisted deposition of silver nanoparticles on a two dimensional support as an inexpensive and highly efficient SERS substrate. RSC Adv 2015;5(46):36368–73.
[26] Cheng Li, Wu H, Li J, Zhao H, Wang L. Polydopamine modified ultrathin hydroxyapatite nanosheets for anti-corrosion reinforcement in polymeric coatings. Corros Sci 2021;178:109064.
[27] Wu R, Yue W, Li Y, Huang A. Ultra-thin and high hydrogen permeable carbon molecular sieve membrane prepared by using polydopamine as carbon precursor. Mater Lett 2021;295:129863.
[28] Dong S, Xiao G, Chen C, Yang Z, Chen C, Wang Q, et al. Polydopamine enwrapped titanium dioxide-assisted dispersion of graphene to strength fire resistance of intumescent waterborne epoxy coating. Prog Org Coat 2021;157:106291.
[29] Sherwood J, Xu YL, Lovas K, Qin Y, Bao YP. Surface functionalization of dopamine coated iron oxide nanoparticles for various surface functionalities. J Magn Magn Mater 2016;427:220–4.
[30] Wu Y, Chen X, Wang X, Yang M, Xu F, Hou C, et al. A fluorescent biosensor based on prismatic hollow Metal-polydopamine frameworks and 6-carboxyfluorescein (FAM)-labeled protein aptamer for CA15-3 detection. Sens Actuators B Chem 2021;329:129249.
[31] Guerrini L, Rodriguez-Loureiro I, Correa-Duarte MA, Lee YH, Ling XY, García de Abajo FJ, et al. Chemical speciation of heavy metals by surface-enhanced Raman scattering spectroscopy: identification and quantification of inorganic- and methyl-mercury in water. Nanoscale 2014;6(14):8368–75.
[32] Sun DD, Hao YH, Fu YM, Ma J. Organic dye concentration monitoring through anoptical microfiber enabled by multiwalled carbon nanotubes. J Opt Soc Am B 2021;38(12):178–85.
[33] Sun D, Xu S, Liu S, Fu Y, Yang Y, Ma J. Real-Time Drug Delivery System Tracked Through an Optical Microfiber: Supporting Interface of Metal-Organic-Framework. Part Part Syst Charact 2022;39(2):2100221.
[34] Sun L-P, Huang T, Yuan Z, Lin W, Xiao P, Yang M, et al. Ultra-high sensitivity of dual dispersion turning point taper-based Mach-Zehnder interferometer. Opt Express 2019;27(16):23103.
[35] Ahsani V, Ahmed F, Jun MBG, Bradley C. Tapered Fiber-Optic Mach-Zehnder Interferometer for Ultra-High Sensitivity Measurement of Refractive Index. Sensors 2019;19(7):1652.
[36] Liu KJ, Fan JH, Luo BB, Zou X,Wu DC,Zou XL, et al. Highly sensitive vibration sensor based on the dispersion turning point microfiber Mach-Zehnder interferometer. Opt Express 2021;29(21): 32983-95.
[37] Huang Y, Tian Z, Sun L-P, Sun D, Li J, Ran Y, et al. High-sensitivity DNA biosensor based on optical fiber taper interferometer coated with conjugated polymer tentacle. Opt Express 2015;23(21):26962.
[38] Shi Se, Wang L, Su R, Liu B, Huang R, Qi W, et al. A polydopamine-modified optical fiber SPR biosensor using electroless-plated gold films for immunoassays. Biosens Bioelectron 2015;74:454–60.
[39] Hu M, Mi BX. Enabling graphene oxide nanosheets as water separation membranes. Environ Sci Technol 2013;47(8):3715–23.
[40] Huang Y, Tao CA, Chen R, Sheng LP, Wang JF. Comparison of Fabrication Methods of Metal-Organic Framework Optical Thin Films. Nanomaterials 2018;8(9):676.
[41] Sureshkumar M, Lee CK. Polydopamine coated magnetic-chitin (MCT) particles as a new matrix for enzyme immobilization. Carbohyd Polym 2010;84(2):775–80.
[42] Mizutani G, Ushioda S. Normal mode analysis of surface adsorbed and coordinated pyridine molecule. J Chem Phys 1989;91(1):598–602.
[43] Du YX, Liu RY, Liu BH, Wang SH, Han MY, Zhang ZP. Surface-enhanced Raman scattering chip for femtomolar detection of mercuric ion (II) by ligand exchange. Anal Chem 2013;85(6):3160–5.
[44] Li K, Liang AH, Jiang CA, Li F, Liu QY, Jiang ZL. A stable and reproducible nanosilver-aggregation-4-mercaptopyridine surface-enhanced Raman scattering probe for rapid determination of trace Hg^{2+}. Talanta 2012;99:890–6.
[45] Chen ZL, Han KL, Zhang YN. Reflective Fiber Surface Plasmon Resonance Sensor for High-Sensitive Mercury Ion Detection. Appl Sci 2019;9(7):1480.
[46] Halkare P, Punjabi N, Wangchuk J, Nair A, Kondabagil K, Mukherji S. Bacteria functionalized gold nanoparticle matrix based fiber-optic sensor for monitoring heavy metal pollution in water. Sens Actuators B Chem 2019;281:643–51.